

PROCEEDINGS OF SPIE

[SPIDigitalLibrary.org/conference-proceedings-of-spie](https://spiedigitallibrary.org/conference-proceedings-of-spie)

Optical absorption, photoionization and binding energy of shallow donor impurity in spherical multilayered quantum dot

Holovatsky, V., Holovatska, N., Chubrei, M.

V. A. Holovatsky, N. H. Holovatska, M. V. Chubrei, "Optical absorption, photoionization and binding energy of shallow donor impurity in spherical multilayered quantum dot," Proc. SPIE 12126, Fifteenth International Conference on Correlation Optics, 1212603 (20 December 2021); doi: 10.1117/12.2614673

SPIE.

Event: Fifteenth International Conference on Correlation Optics, 2021, Chernivtsi, Ukraine

Optical absorption, photoionization and binding energy of shallow donor impurity in spherical multilayered quantum dot

Holovatsky V.A., Holovatska N.H., Chubrei M.V.
Chernivtsi National University, 2 Kotsubynsky str., Chernivtsi, Ukraine, 58012

ABSTRACT

Energy spectrum, wave functions and binding energies of the electron to the donor impurity ion located in the center of a multilayer spherical quantum dot (MSQD) consisting of a core (GaAs) and two spherical shells ($\text{Al}_x\text{Ga}_{1-x}\text{As}$ and GaAs) were studied within the effective mass approximation. The magnetic field influence on the energy spectrum and wave functions of the electron is calculated by the diagonalization method. It is shown that the decrease of the external shell thickness as well as the increase of the magnetic field induction changes the electron localization in the nanosystem and it significantly affects the binding energy of the electron with the impurity, photoionization cross section (PCS) and intersubband absorption coefficient. The position of the PCS peak associated with the quantum transition of an electron from the ground state to the $1p^0$ state shifts to the region of higher energies, and its height decreases. At the same time, the height of PCS peaks associated with quantum transitions to higher excited states increases.

Keywords: multilayer quantum dot, donor impurity, photoionization cross section, absorption coefficient.

INTRODUCTION

Multilayer spherical quantum dots (MSQD) consisting of a core and several shells of semiconductor materials with different bandgap values are intensively studied due to the prospects of their use in various nanoelectronics and nanophotonics devices such as white light sources, high-efficiency photovoltaic devices, fluorescent labels with multimode radiation, various detectors, magneto-optical devices and memory elements for novel computers¹⁻⁵.

The creation of semiconductor devices requires theoretical studies of the MSQD optical properties, the influence of impurities and external fields on their energy spectrum. Most of such studies are based on solutions of the one-particle Schrödinger equation within the effective mass approximation. To find the energies of several lowest states, researchers often use different variational methods or the method of perturbation theory⁶⁻¹⁶, the potential morphing method¹⁷⁻¹⁹ or numerical finite element method²⁰⁻²³. The effect of charged impurities and external fields on the MSQD optical properties was also investigated by the matrix (diagonalization) method²⁴⁻³².

The calculation of the energy spectrum and wave functions (WF) of an electron in spherical nanosystems with an impurity by the diagonalization method requires consideration of a large number of terms due to the presence of a singular potential. The diagonalization of such matrices encounters technical problems of solution stability.

For the case of a central impurity, this problem is solved by using exact solutions of the Schrödinger equation based on Mathieu and Whittaker functions, degenerate hypergeometric or Coulomb wave functions³³⁻³⁷. Their numerical calculation is more complicated than the Bessel functions, but the use of an orthonormal basis on Coulomb WFs decreases the size of the matrix required for diagonalization when studying the effect of electric or magnetic field on the impurity states in MSQD.

The similar orthonormal WF basis was used to study the magnetic field effect on the optical properties of spherical nanosystems of the core/shell type (MSQD with a single potential well)³⁸. The impurity binding energy and the oscillator strength of quantum transitions in MSQD with two potential wells separated by potential barrier were studied using the exact solutions of the Schrödinger equation based on degenerate hypergeometric functions^{37, 39}.

Studies of MSQDs with two and three wells^{30, 40} show that a strong constant magnetic field reduces the effective width of the outer potential well which leads to changes in the electron localization in the ground and excited states and, thus, affects the dipole moment and the oscillator force of quantum transitions.

To increase the sensitivity of the nanosystem optical properties to the magnetic field, it is necessary to fit such MSQD core and shell size that the electron in the ground state is localized in the outer shell but transits into the inner shell upon a small decrease of the shell size⁴¹.

The intersubband absorption coefficient and PCS are those optical characteristics that were intensely studied for simple spherical and cylindrical QDs and MSQDs with various profiles of confinement potential^{10-14, 16-19, 32}. The electric³² and magnetic⁴² field effect on the PCS of the central and off-center donor impurity in the spherical shell which forms a potential well of finite depth was investigated by the diagonalization method using an orthonormal basis of Bessel functions. The need of taking into account quantum transitions to higher excited states was shown as their contribution grows with increasing external perturbation. Similar effects for MSQD with two wells were not studied.

Here, we report the effect of the outer potential well width of the GaAs/Al_xGa_{1-x}As/GaAs MSQD with a central donor impurity and magnetic field on the energy spectrum, wave functions, binding energy, impurity photoionization cross-section and intersubband optical absorption coefficient. We prove that the effect of an external magnetic field on the light absorption coefficient in MSQD is equivalent to a decrease in the size of the external potential well of the nanosystem.

THEORY

The multilayer spherical quantum dot investigated in this work consists of a spherical core GaAs and two spherical shells (Al_xGa_{1-x}As and GaAs) placed in a wide-gap medium. The core radius is r_0 , the thickness of the spherical layers are Δ_1 and Δ_2 . The MSQD core and the outer spherical shell form two potential wells for the electron, and the inner layer is a potential barrier with height V . The donor impurity is located in the center of the nanosystem core. The scheme of the electron potential energy in MSQD is shown in Fig.1.

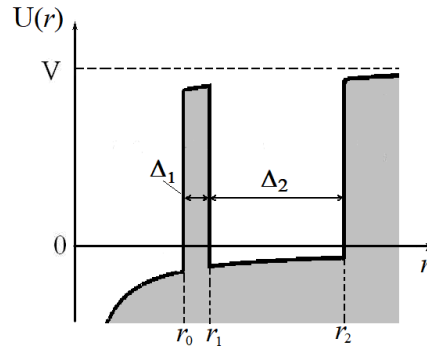


Figure 1. Electron potential energy in GaAs/Al_xGa_{1-x}As/GaAs MSQD at $Z = 1$.

The Schrödinger equation for the electron has the form

$$-\frac{\hbar^2}{2} \vec{\nabla} \frac{1}{\mu(r)} \vec{\nabla} \Psi_{nlm}(\vec{r}) + [U(r) - \frac{Ze^2}{\varepsilon(r)r}] \Psi_{nlm}(\vec{r}) = E_{nl} \Psi_{nlm}(\vec{r}), \quad (1)$$

where the coordinate dependences of the effective mass, dielectric constant and potential energy are expressed as

$$\mu(r) = m_e \begin{cases} m_0, & r \leq r_0, r_1 < r \leq r_2, \\ m_1, & r_0 < r \leq r_1, \end{cases}, \quad \varepsilon(r) = \begin{cases} \varepsilon_0, & r \leq r_0, r_1 < r \leq r_2 \\ \varepsilon_1, & r_0 < r \leq r_1, \end{cases} \quad (2)$$

where m_e is the free electron mass.

$$U(r) = \begin{cases} 0, & r \leq r_0, r_1 < r < r_2, \\ V, & r_0 < r \leq r_1, \\ \infty, & r \geq r_2, \end{cases} \quad (3)$$

Making Eq. (1) dimensionless by using the Rydberg energy $Ry = m_e e^4 / 2\hbar^2$ as a unit of energy and the Bohr radius $a_B = \hbar^2 / m_e e^2$ as a unit of length, and taking into account the spherical symmetry of problem, the equation for the radial part of the wave function is expressed as

$$-\frac{1}{m_0} \left[\frac{\partial^2}{\partial r^2} + \frac{2}{r} \frac{\partial}{\partial r} - \frac{l(l+1)}{r^2} \right] R_{nl}(r) - \frac{2Z}{\varepsilon_0 r} R_{nl}(r) = E_{nl} R_{nl}(r), \quad r \leq r_0, r_1 < r \leq r_2, \quad (4)$$

$$-\frac{1}{m_1} \left[\frac{\partial^2}{\partial r^2} + \frac{2}{r} \frac{\partial}{\partial r} - \frac{l(l+1)}{r^2} \right] R_{nl}(r) + \left(V - \frac{2Z}{\varepsilon_1 r} \right) R_{nl}(r) = E_{nl} R_{nl}(r), \quad r_0 < r \leq r_1 \quad (5)$$

The solutions of (3) and (4) contain the degenerate hypergeometric functions of the 1st and 2nd kind $F(a, b, z)$ and $G(a, b, z)$:

$$R_{nl}(r) = \begin{cases} A_0 e^{-\frac{\xi_0 r}{2}} r^l F(l+1-\eta_0, 2l+2, \xi_0 r), & r \leq r_0 \\ A_1 e^{-\xi_1 r/2} r^l [F(l+1-\eta_1, 2l+2, \xi_1 r) + B_1 G(l+1-\eta_1, 2l+2, \xi_1 r)], & r_0 < r \leq r_1, \\ A_2 e^{-\xi_0 r/2} r^l [F(l+1-\eta_0, 2l+2, \xi_0 r) + B_2 G(l+1-\eta_0, 2l+2, \xi_0 r)], & r_1 < r \leq r_2, \end{cases} \quad (6)$$

$$\xi_0 = -2 \text{sign}(E_{nl}) \sqrt{m_0(-E_{nl})}, \quad \eta_0 = \frac{2Zm_0}{\varepsilon_0 \xi_0}, \quad \xi_1^{e,h} = 2 \text{sign}(V - E_{nl}) \sqrt{m_1(V - E_{nl})}, \quad \eta_1 = \frac{2Zm_1}{\varepsilon_1 \xi_1}, \quad (7)$$

where $\text{sign}(x)$ is a sign function that provides a single analytical form of WF for states with different signs of electron energy. The unknown coefficients and the energy spectrum are determined from the Ben-Daniel-Duke boundary conditions³⁹. The binding energy of the electron and the impurity in the state (nl) can be obtain in the form $E_{nl}^b = E_{nl}^{Z=0} - E_{nl}^{Z=1}$. Based on the energy spectrum and wave functions the effective photoionization cross-section are calculated by the formulas:

$$\sigma(\hbar\omega) = \frac{4\pi^2}{3n_r} \left(\frac{F_{eff}}{F_0} \right)^2 \beta_{FS} \hbar\omega \sum_n |\langle R_{n1}^{Z=0} | r | R_{10}^{Z=1} \rangle|^2 \delta(E_{n1} - E_{10} - \hbar\omega), \quad (8)$$

where $\delta(E) = \Gamma [\pi(E^2 + \Gamma^2)]^{-1}$, $\hbar\omega$ is the photon energy, n_r is the refraction index, $\beta_{FS} = 1/237$ is the fine structure constant, the ratio $F_{eff}/F_0 \approx 1$, $\Gamma = 0.4 \text{ meV}^{32}$. Optical absorption coefficient was calculated for the cases of presence ($Z = 1$) and absence of impurities ($Z = 0$) according to the formula²⁷

$$\alpha(\hbar\omega) = 4\pi\beta_{FS} \sum_n \frac{|(R_{n1}|r|R_{10})|^2 \rho \hbar\omega \Gamma_0}{(E_{n1} - E_{10} - \hbar\omega)^2 + (\hbar\Gamma_0)^2}, \quad (9)$$

where $\rho = 1/V$ is the carrier density in MSQD, $\Gamma_0 = 1/\tau_0$, $\tau_0 = 0.14 \text{ ps}$ is the relaxation time²⁷.

The study the magnetic field influence on the optical absorption coefficient needs to solve the Schrödinger equation

$$\left(\vec{p} - \frac{e}{c} \vec{A} \right) \frac{1}{2\mu(r)} \left(\vec{p} - \frac{e}{c} \vec{A} \right) \Psi_f(\vec{r}) + [U(r) - \frac{Ze^2}{\varepsilon(r)r}] \Psi_f(\vec{r}) = E_f \Psi_f(\vec{r}). \quad (10)$$

The electron wave functions in MSQD placed in a magnetic field are calculated by matrix method^{40,41} using the expansion

$$\Psi_{jm}(\vec{r}) = \sum_{n,l} c_{nl}^{jm} \psi_{nlm}(\vec{r}), \quad (11)$$

where $\psi_{nlm}(\vec{r}) = R_{nl}(r) Y_{lm}(\theta, \phi)$.

To determine the coefficients c_{nl}^{jm} and electron energy spectrum we obtain the secular equation $|H_{nl,n'l'} - E_{jm} \delta_{n,n'} \delta_{l,l'}| = 0$.

The eigenvalues (E_{jm}) and eigenvectors (c_{nl}^{jm}) of the matrix $H_{nl,n'l'}$ determine the energy spectrum and the wave functions of an electron in MSQD driven by the magnetic field⁴¹.

RESULTS AND DISCUSSION

The following physical parameters of MSQD were used in numerical calculations¹⁶: $x=0.3$, $m_0=0.067$, $m_1=0.092$, $\varepsilon_0=13.18$, $\varepsilon_1=12.24$, $V = 248 \text{ meV}$, $r_0=10 \text{ nm}$, $\Delta_1=2 \text{ nm}$. The dependence of the electron energy spectrum in MSQD on Δ_2 is shown in

Fig. 2. In the absence of impurities, at small values of $\Delta_2 < r_0$ the electron is localized in the nanosystem core as shown by the horizontal region of the E_{10} (Δ_2) dependence, and at $\Delta_2 > r_0$ the electron is located in the outer potential well where its energy is less. The change in the electron localization occurs in the region of energy levels E_{10} and E_{20} anticrossing ($\Delta_2 \sim 10$ nm). In the presence of impurity (Fig. 2a) the region of the anticrossing is shifted to $\Delta_2 \sim 14$ nm.

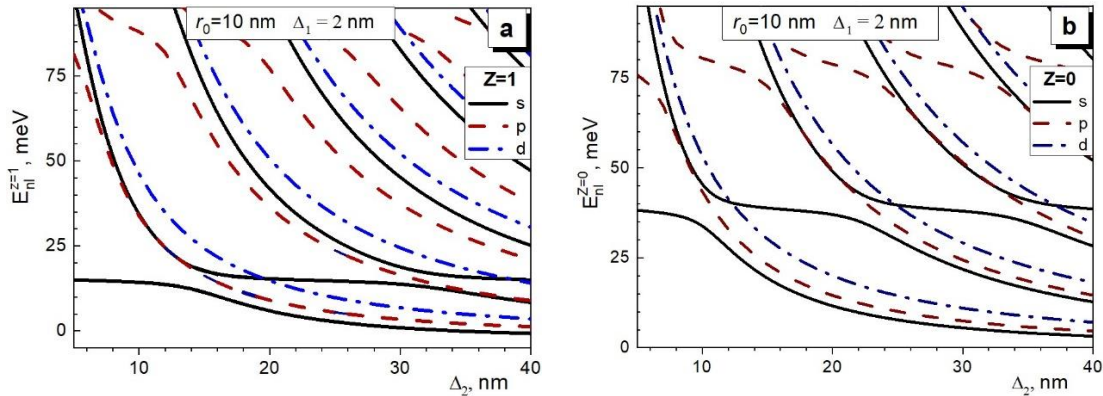


Figure 2. Dependence of the electron energy spectrum on Δ_2 at $r_0 = 10$ nm and $\Delta_1 = 2$ nm (a – $Z = 1$, b – $Z = 0$).

The radial distribution of electron density $w(r) = |R_{nl}(r)|^2 r^2$ in the ground (1s) and excited states (1p, 2p) that participate in quantum transitions and determine the nanosystem optical properties is presented in Fig. 3. The dimensions of the outer potential well which correspond to the beginning ($\Delta_2 = 12$ nm) and the end ($\Delta_2 = 18$ nm) of the anticrossing region are selected for the display.

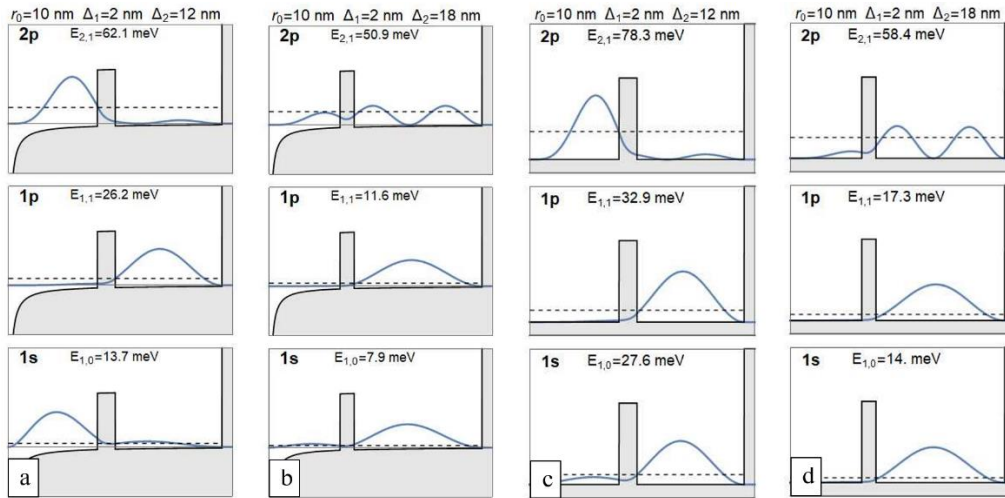


Figure 3. Distribution of electron density in 1s, 1p, 2p states: ($Z = 1$) a – $\Delta_2 = 12$ nm, b – $\Delta_2 = 18$ nm; ($Z = 0$) c – $\Delta_2 = 12$ nm, d – $\Delta_2 = 18$ nm.

One can estimate the electron binding energy to the impurity in s and p states from values energies of this states in nanosystem with and without impurity. The maximum values of the electron binding energy to the impurity correspond to the case of electron localization in the nanosystem core.

The photon energy dependences of impurity PCS $\sigma(\hbar\omega)$ at various values of Δ_2 are plotted in Fig. 4. The main contributor to the PCS at $\Delta_2 = 20$ nm is the quantum transition $1s-1p^0$ which is confirmed by the overlap of the corresponding WFs (Fig. 3 b, d). As the size of the outer potential well decreases, the electron in 1s and $2p^0$ states localizes in the core. Therefore, the first

PCS peak ($1s-1p^0$) decreases and the second PCS peak associated with the $1s-2p^0$ quantum transition increases. Additionally, upon decreasing Δ_2 all PCS peaks are shifted to the region of higher energies.

The dependence $\alpha(\hbar\omega)$ is shown in Fig. 3b. Unlike PCS, the expression for OAC contains the dipole moment of the quantum transition between states at $Z = 1$ (in the presence of impurity) or at $Z = 0$ (in the absence of impurity). But the qualitative behavior of absorption peaks with decreasing Δ_2 value is somewhat similar to PCS, i.e. a shift of peaks to the region of higher energies and an increase in the value of peaks of higher excited states.

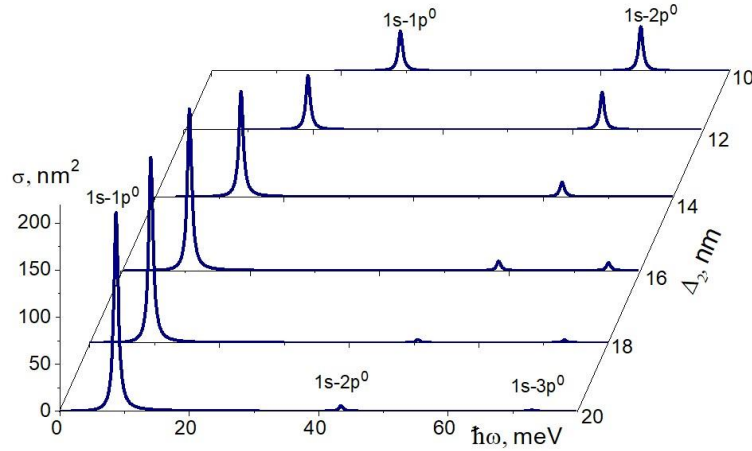


Figure 4. Spectral dependences $\sigma(\hbar\omega)$ at various value Δ_2 .

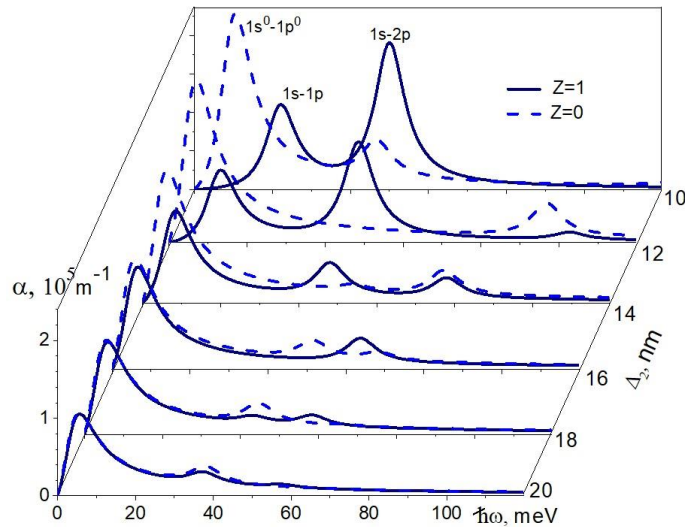


Figure 5. Photon energy dependences of optical absorption coefficient at various value Δ_2 .

Obtained changes in the spectral dependences $\sigma(\hbar\omega)$ and $\alpha(\hbar\omega)$ caused by the reduction of the outer potential well allow us to predict the effect of the external constant magnetic field on the MSQD optical characteristics. Increasing of the magnetic field induction reduces the electron cyclotron radius $r_c = \sqrt{2\hbar/eB}$. If this becomes smaller than the MSQD radius, the magnetic field will increase the confinement and decrease the effective potential well width in the direction perpendicular to the magnetic field. The change of the electron localization under the selected MSQD dimensions will require $\sim 10-15$ T induction of the magnetic field ($r_c \approx 90/\sqrt{B}$ nm).

The magnetic field effect on the electron energy spectrum in MSQD with impurity ($m=0$) is shown in Fig.6. The electron wave functions are shown for the points $B=10\text{T}$ and $B=20\text{T}$. The energies of all electron states increase with magnetic field induction growth. It is like to the decrease of outer potential well (Fig. 2).

The magnetic field effect on the light absorption coefficient of MSQD with impurity ($m=0$) is shown in Fig.7. The absorption peak $1s-1p$ becomes lower and $1s-2p$ peak becomes higher as magnetic field is stronger. A similar evolution of light situation is observed in the Fig.5.

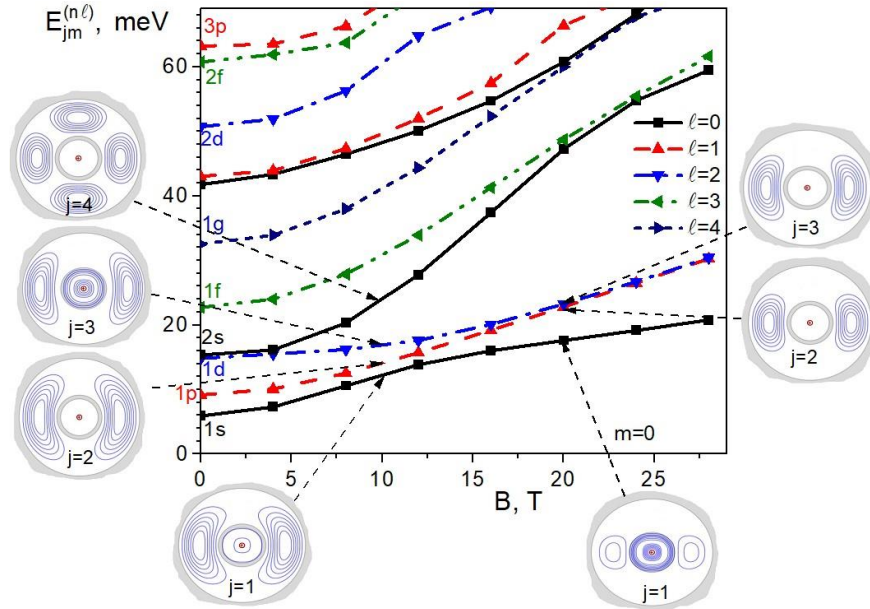


Figure 6. Dependence of electron energy spectrum on magnetic field induction ($Z=1$).

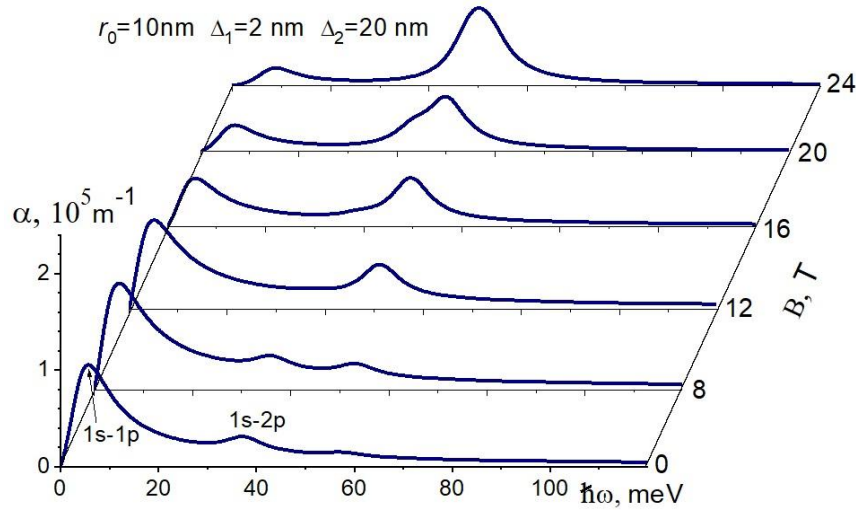


Figure 7. Evolution of the spectral dependence of light absorption coefficient in magnetic field ($Z=1$).

CONCLUSIONS

The exact solutions of the Schrödinger equation for the electron in a GaAs/Al_xGa_{1-x}As/GaAs MSQD with central impurity were obtained. The impurity photoionization cross-section and the intersubband absorption coefficient were investigated on the basis of the energy spectrum and wave function of the electron for various values of the outer potential well size. It was shown that in the region of the energy levels anticrossing the nanosystem is most sensitive to the effect of impurity and external fields on its optical characteristics. A decrease of the outer potential well size of MSQD leads to the shift of PCS and OAC peaks to the high-energy region and to an increase in the contribution of quantum transitions to higher excited states to the optical characteristics. At the absence of impurity in MSQD intersubband absorption occurs mainly through the quantum transition $1s^0-1p^0$, whereas in the presence of a central impurity the greatest absorption occurs at higher photon energy through the quantum transition $1s-2p$. It is shown that the magnetic field with induction of 10-15 T influences the nanosystem optical characteristics as well as the reducing of the outer shell thickness does.

REFERENCES

- [1] Zhang, Z., "Dual Emissive Cu:InP/ZnS/InP/ZnS Nanocrystals: Single-Source 'Greener' Emitters with Flexibly Tunable Emission from Visible to Near-Infrared and Their Application in White Light-Emitting Diodes", *Chem. Mater.* 27. – P.1405–1411 (2015).
- [2] Rudko, G. Yu., Fediv, V. I., Davydenko, I., Gule, E. G., Olar, O., Kovalchuk, A. O., "Synthesis of Capped AIBVI Nanoparticles for Fluorescent Biomarkers", *Nanoscale Research Letters* 11. – P. 83 (2016).
- [3] Chatterjee, K., Sarkar, S., Jagajjanani, Rao K., Paria, S., "Core/shell nanoparticles in biomedical applications", *Adv Colloid Interf Sci.* 209:8–39 2 (2014).
- [4] Lahon, S., Jha, P. K., & Mohan, M. "Nonlinear interband and intersubband transitions in quantum dots for multiphoton photodetectors", *Journal of Applied Physics* 109, 5 (2011).
- [5] Jiao, S., Shen, Q., Mora-Seró, I., Wang, J., Pan, Z., Zhao, K., Kuga, Y., Zhong, X., Bisquert, J., "Band engineering in core/shell ZnTe/CdSe for photovoltage and efficiency enhancement in exciplex quantum dot sensitized solar cells", *ACS Nano*, 9(1), 908–915 (2015).
- [6] Yuan, J.-H., Xie, W.-F., He, L.-L., "Shallow donor impurity ground state in a GaAs/AlAs spherical quantum dot within an electric field", *Commun. Theor. Phys.* 52, 710–714 (2009).
- [7] Xie, W., "Impurity effects on optical property of a spherical quantum dot in the presence of an electric field", *Physica B*, 405, 3436–3440 (2010).
- [8] Sadeghi, E., "Electric field and impurity effects on optical property of a three-dimensional quantum dot: a combinational potential scheme", *Superlattice and Microstructures.* 50, 331–339 (2011).
- [9] Dane C., Akbas H., Guleroglu A., Minez S., Kasapoglu K., "The hydrostatic pressure and electric field effects on the normalized binding energy of hydrogenic impurity in a GaAs/AlAs spherical quantum dot", *Phys. E:* 44, 186–189 (2011).
- [10] Burileanu, L. M., "Photoionization cross-section of donor impurity in spherical quantum dots under electric and intense laser fields", *J. Lumin.* 145, 684–689 (2014).
- [11] Corella-Madueno, Rosas, R., Marin, J. L., Riera, R., "Hydrogenic impurity in spherical quantum dots in a magnetic field", *J. Appl. Phys.* 90, 2333–2337 (2001).
- [12] Feddi, E., Talbi, A., Mora-Ramos, M. E., El Haouari M., Dujardin, F., Duque, C. A., "Linear and nonlinear magneto-optical properties of an off-center single dopant in a spherical core/shell quantum dot", *Physica B* 524, 64–70 (2017).
- [13] Barseghyan M., Kirakosyan, A., Duque, C. A., "Donor-impurity related binding energy and photoionization cross-section in quantum dots: electric and magnetic fields and hydrostatic pressure effects", *Eur. Phys. J. B* 72, 521–529 (2009).
- [14] Li, S., Shi, L., Yan, Z.-W., "Binding energies and photoionization cross-sections of donor impurities in GaN/Al_xGa_{1-x}N spherical quantum dot under hydrostatic pressure", *Mod. Phys. Lett. B* 34, 2050153 (2020).
- [15] Holovatsky, V. A., Frankiv, I. B., "Oscillator strength of quantum transition in multi-shell quantum dots with impurity", *J. Optoelectron Adv. M.*, 15, 1–2 (2013).
- [16] Boz, F. K., Aktas, S., Bilekkaya, A., Okan, S. E., "The multilayered spherical quantum dot under a magnetic field", *Applied Surface Science*, 256(12), 3832–3836 (2010).

- [17] Karabulut, I., Baskoutas, S. “Linear and nonlinear optical absorption coefficients and refractive index changes in spherical quantum dots: Effects of impurities, electric field, size, and optical intensity”, *J. Appl. Phys.*, 103(7), 1–6 (2008).
- [18] Zeng, Z., Garoufalos, C. S., Baskoutas, S., Terzis, A. F., “Stark effect of donor binding energy in a self-assembled GaAs quantum dot subjected to a tilted electric field”, *Phys. Lett. A: Gen. At. Solid State Phys.*, 376(42–43), 2712–2716 (2012).
- [19] Zeng, Z., Garoufalos, C., Terzis, A., Baskoutas, S., “Linear and nonlinear optical properties of ZnO/ZnS and ZnS/ZnO core shell quantum dots: Effects of shell thickness, impurity, and dielectric environment”, *J. Appl. Phys.*, **114**, 023510 (2013).
- [20] Cristea M., Niculescu, E., “Hydrogenic impurity states in CdSe/ZnS and ZnS/CdSe core-shell nanodots with dielectric mismatch”, *Eur. Phys. J. B*, 85, 6 (2012).
- [21] Niculescu, E. C., Stan, C., Cristea, M., Truscă, C., “Magnetic-field dependence of the impurity states in a dome-shaped quantum dot”, *Chemical Physics*, 493, 32–41 (2017).
- [22] Cristea, M., “Simultaneous effects of electric field, shallow donor impurity and geometric shape on the electronic states in ellipsoidal ZnS/CdSe core-shell quantum dots”, *Phys. E: Low-Dimens. Syst. Nanostructures*, 103, 300–306 (2018).
- [23] Heyn, C., Duque, C. A. “Donor impurity related optical and electronic properties of cylindrical GaAs-Al_xGa_{1-x}As quantum dots under tilted electric and magnetic fields”, *Scientific Reports*, 10(1), 1–18 (2020).
- [24] Çakir, B., Atav, U., Yakar, Y., Özmen, A., “Calculation of Zeeman splitting and Zeeman transition energies of spherical quantum dot in uniform magnetic field”, *Chem. Phys.* 475, 61–68 (2016).
- [25] Liu, D.-M., Xie, W.-F., “Binding energy of an off-center D – in a spherical quantum dot”, *Commun. Theor. Phys.* 51, 919–922 (2009).
- [26] Al, E. B., Kasapoglu, E., Sakiroglu, S., Sari, H., Sökmen, I., Duque, C. A., “Binding energies and optical absorption of donor impurities in spherical quantum dot under applied magnetic field”, *Physica E* 119, 114011 (8pp) (2020).
- [27] Al, E. B., Kasapoglu, E., Sari, H., & Sökmen, I., “Optical properties of spherical quantum dot in the presence of donor impurity under the magnetic field”, *Physica B: Condensed Matter*, 613(March) (2021).
- [28] Boichuk, V. I., Bilynskiy, I. V., Leshko, R. Y., Turyanska, L. M., “The effect of the polarization charges on the optical properties of a spherical quantum dot with an off-central hydrogenic impurity”, *Physica E* 44, 476–482 (2011).
- [29] Holovatsky, V., Yakhnevych, M., Voitsekhivska, O., “Optical properties of GaAs/Al_xGa_{1-x}As/GaAs quantum dot with off-central impurity driven by electric field”, *Condens. Matter Phys.* 21, 13703 (9pp) (2018).
- [30] Holovatsky, V., Bernik, I., Yakhnevych, M. “Effect of magnetic field on energy spectrum and localization of electron in CdS/HgS/CdS/HgS/CdS multilayered spherical nanostructure”, *Physica B* 508, 112-117 (2017).
- [31] Holovatsky, V., Voitsekhivska, O., Yakhnevych, M., “The effect of magnetic field and donor impurity on electron spectrum in spherical core-shell quantum dot”, *Superlattices and Microstructures* 116, 9-16 (2018).
- [32] Holovatsky, V., Chubrey, M., Voitsekhivska, O., “Effect of electric field on photoionisation cross-section of impurity in multilayered quantum dot”, *Superlattices and Microstructures* 145, 106642 (9pp) (2020).
- [33] Baimuratov, A. S., Rukhlenko, I. D., Turkov, V. K., Ponomareva, I. O., Leonov, M. Y., Perova, T. S., Berwick, K., Baranov, A. V., “Level anticrossing of impurity states in semiconductor nanocrystals. *Scientific Reports*”, 4, 1–6 (2014).
- [34] Boichuk, V. I., Bilynskiy, I. V., Leshko, R. Y., “Hole, impurity and exciton states in a spherical quantum dot”, *Condensed Matter Physics*, 13(1), 13702–13713 (2010).
- [35] Naimi, Y., Jafari, A. R., “Oscillator strengths of the intersubband electronic transitions in the multi-layered nano-antidots with hydrogenic impurity”, *Journal of Computational Electronics*, 11(4), 414–420 (2012).
- [36] Kostić, R., Stojanović, D., “Electric field effect on the nonlinear and linear intersubband absorption spectra in CdTe/ZnTe spherical quantum dot”, *Journal of Nanophotonics*, 6(1), 061606–1 (2012).
- [37] Mikhail, I. F. I., El Sayed S. B. A., “Exact and variational calculations of a hydrogenic impurity binding energy in a multilayered spherical quantum dot”, *Physica E: Low-Dimensional Systems and Nanostructures* 43 (7) 1371-1378 (2011).
- [38] Rahimi, F., Ghaffary, T., Naimi, Y., Khajehazad, H., “Optical and Quantum Electronics Effect of magnetic field on energy states and optical properties of quantum dots and quantum antidots”, *Opt. Quantum Electron.*, 53, 47 (2021).
- [39] Holovatsky V., Bernik I., Voitsekhivska O. Oscillator strengths of quantum transitions in spherical quantum dot GaAs/Al_xGa_{1-x}As/GaAs/Al_xGa_{1-x}As with on-center donor impurity. *Acta Physica Polonica A*, 125, 1 (2014).
- [40] Holovatsky, V., Voitsekhivska, O., Yakhnevych, M., “Effect of magnetic field on an electronic structure and intraband quantum transitions in multishell quantum dots”, *Phys. E: Low-Dimens. Syst. Nanostructures*, 93, 295–300 (2017).
- [41] Holovatsky, V., Bernik, I., Yakhnevych, M., “Effect of magnetic field on electron spectrum and probabilities of intraband quantum transitions in spherical quantum-dot-quantum-well”, *Phys. E: Low-Dimens. Syst. Nanostructures*, 83 (2016).